

Application of the Transmission Line Matrix Method to the Shielding Effectiveness Analysis of Metallic Enclosures

A.R. Attari¹, K. Barkeshli*, F. Ndagijimana² and J. Dansou²

In this paper, the Transmission Line Matrix (TLM) method is used for the electromagnetic characterization of the Shielding Effectiveness (SE) of rectangular enclosures with apertures of arbitrary shape. Applying suitable Hanning windows in the time domain drastically reduces the number of time steps required to model the coupling behavior of resonant enclosures. Comparison of the numerical results with available measured data shows that the method is an efficient and accurate technique to evaluate the shielding effectiveness of metallic shields in the time domain and over a wide frequency range. The proposed method can be used as an intermediate design tool for the evaluation of the effects of various aperture shapes on the effectiveness of shield assemblies.

INTRODUCTION

Electromagnetic shielding is frequently used to either reduce emission or improve the immunity of electronic equipment to interference. The ability of an enclosure to perform this task is characterized by its Shielding Effectiveness (SE), which is defined as the ratio of the field in the presence of the enclosure to that in its absence. It is an important parameter that affects the electromagnetic compatibility of equipments. The SE of a metal enclosure is determined mainly by its general shape and the shape of its apertures.

Stringent EMC regulatory requirements make the efficient analysis of shielding effectiveness very important in the development of new high frequency circuits. EMI/EMC analyses typically involve a very wide band of frequency. This creates the immense challenge of developing numerical models that remain reasonably accurate over a wide frequency band.

Shielding effectiveness can be calculated by classical analytical techniques or by numerical simulation. Analytical formulations provide a faster mean of esti-

imating SE. However, since these methods are based on simplifying assumptions, they cannot provide sufficient accuracy to meet the design specifications when the shielding structure is geometrically complex. A number of computational methods have been proposed for the solution of shielding problems, including the TLM method [1], the Finite-Difference Time-Domain (FD-TD) method [2], the Method of Moments (MoM) [3] and the Finite Element Method (FEM) [4].

In this paper, an efficient method is presented for the analysis of shielding effectiveness in high frequency communication circuits. It is based on the Transmission Line Matrix (TLM) method. Since the formulation is in the time domain, wide band effects are easily and accurately modeled. Comparison of the results obtained from the proposed numerical method with those obtained from measurements, show that the TLM method gives more accurate results than other methods reported in the literature. The computational aspects for increased efficiency are also considered.

The fundamentals of the TLM method, as well as its advantages and limitations, are briefly discussed in the next section. Then, the configuration of the problem and the results of TLM simulation are demonstrated. The emphasis will be on important aspects that have been considered in the TLM analysis. The effects of various aperture shapes on the shielding effectiveness of the rectangular enclosures are presented in the last section.

1. Department of Electrical Engineering, Sharif University of Technology, Tehran, I.R. Iran.

*. Corresponding Author, Department of Electrical Engineering, Sharif University of Technology, Tehran, I.R. Iran.

2. LEMO/IMEP - ENSERG/UJF, 23 rue des Martyrs, BP 257, 38016, Grenoble, Cedex 1, France.

TLM METHOD

Transmission Line Matrix (TLM) method is a time domain differential method, based on modeling fields by analogy to voltages and currents in a network of transmission lines. The basic computational cell of the TLM, representing propagation in a block of space, is the node, which consists of six interconnected lines. Figure 1 depicts the most commonly used Symmetrical Condensed Node (SCN) introduced by Johns [5]. The stubs in this node take into account different material properties as well as the non-cubic blocks of space. A non-cubic cell is used in a graded mesh. The time-step used in the calculations is related to the absolute dimensions of the node and also to the ratio of three dimensions of each node. At each time-step, twelve pulses, V^i , are incident at the ports of each node and are scattered according to the theory of transmission lines to produce twelve reflected pulses:

$$V^r = [S].V^i, \tag{1}$$

where $[S]$, the TLM scattering matrix, is a 18×18 matrix. The reflected pulses at time-step k become the new incident pulses at adjacent cells at time-step $k + 1$. At each time-step, all field components may be obtained at each node directly from the voltage pulses. The TLM method offers complete time-domain information over the entire problem region and is suitable for finding the transient time response. Results in the frequency domain may be obtained by simply taking the Fourier transform of the results in the time-domain. The TLM is a local method which, therefore, makes it very simple to solve inhomogeneous problems or problems with complex structures.

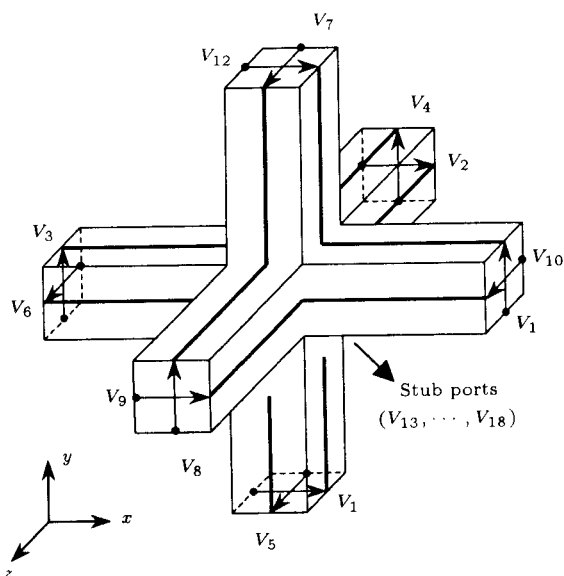


Figure 1. A symmetrical condensed node.

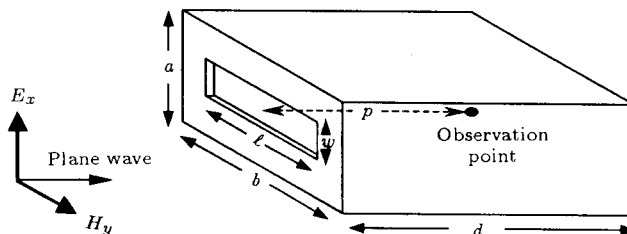


Figure 2. A typical enclosure configuration.

In some problems (such as the SE of an enclosure), the approach to steady-state may be slow and require many time-steps. Successful simulations, therefore, hinge on controlling demands on computational resources, while maintaining reasonable accuracy.

DEFINITION OF THE PROBLEM

Figure 2 shows a typical metallic enclosure with a rectangular aperture of dimension $w \times l$ illuminated by a plane wave. All sides are assumed perfectly conducting with a thickness, t . The observation point is located at a distance, p , away from the aperture inside the enclosure and on a line normal to the aperture and passing through the center of the enclosure. The thickness, t , the side lengths, w and l , and the distance, p are variables in different simulations. The enclosure is excited by a plane wave of unit amplitude $E_x = 1$ V/m.

The shielding effectiveness, SE, is defined as the ratio of E_x , at the observation point in the presence of the enclosure, to that in its absence:

$$SE = 20 \log \frac{E_{x0}}{E_{x1}}, \tag{2}$$

where E_{x0} and E_{x1} are the values of E_x in the absence of the enclosure and in its presence, respectively.

NUMERICAL RESULTS

Consider the metallic enclosure shown in Figure 2. The internal dimensions of enclosures are assumed to be $a = 120$ mm and $b = d = 300$ mm. This enclosure has been studied in the literature [4,6,7]. In addition to the enclosure, the free space around the enclosure must be modeled. The free space region is kept as small as possible to minimize the size of the computational region. For all simulations, a free space volume of $120 \text{ mm} \times 300 \text{ mm} \times 100 \text{ mm}$ is placed in front of the aperture. A simple absorbing boundary condition is applied in the free space region. At least four nodes were found necessary to accurately predict the effect of aperture width.

As a first example, consider a $5 \text{ mm} \times 100 \text{ mm}$ aperture. A uniform mesh was used, resulting in a TLM cell size of $\Delta l = 2.5$ mm. Hence, the time step is

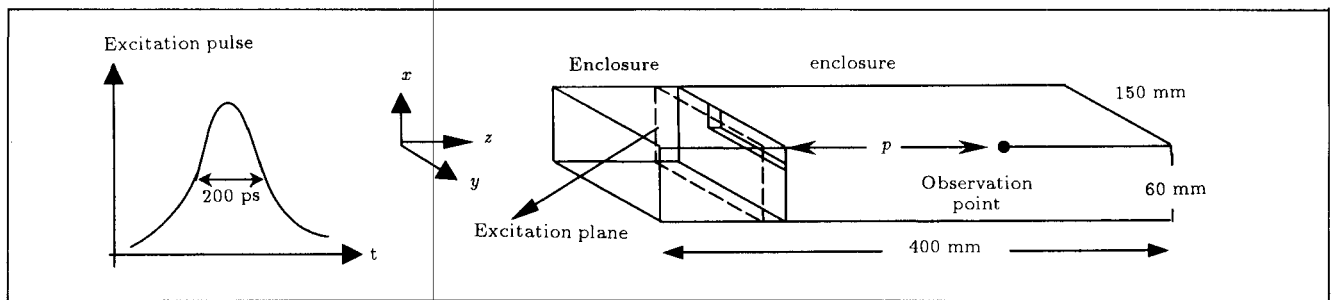


Figure 3. The simulated region including a quarter of the enclosure.

set at:

$$\Delta t = \frac{\Delta l}{2c} = 4.167ps, \quad (3)$$

where $c = 3 \times 10^8$ m/s is the speed of light. The selected cell size $\Delta l < (\lambda/10)$ implies that the dispersion error is negligible up to 12 GHz. However, for illustrative purposes, the results are reported only up to 1 GHz.

To minimize processing requirements, the symmetry shown in Figure 2 can be used to advantage. Perfectly electric and magnetic conducting walls are placed at $x = a/2$ and $y = b/2$ symmetry planes, respectively. Thus, only a quarter of the structure needs to be solved, as shown in Figure 3, and the necessary memory and processing time required will be reduced by a factor of four. The total size of the simulated region is, thus, 60 mm \times 150 mm \times 400 mm with an overall number of 24 \times 60 \times 160 nodes.

The incident wave is assumed to be a 200 ps Gaussian pulse and the time-domain output at the observation point is extracted by the TLM method. In order to reduce the undesired reflections from the absorbing boundary, the plane of excitation is placed very close to the aperture (1.5 Δl away before the aperture), as shown in Figure 3.

Taking the Fourier transform of the output and the excitation, the spectral behavior of the shielding effectiveness can be calculated from Equation 2. First, a simple rectangular window is applied to the time-domain response of the enclosure and aperture with the duration of $T_1 = 833$ ns. The time-domain response of the TLM for an enclosure of thickness $t = 2.5$ mm is depicted in Figure 4. The shielding effectiveness for 200,000 and 500,000 iterations is shown in Figure 5. These results show errors in low frequency range as well as an ambiguity in the spectral values of SE.

The numerical complication in the analysis is amplified by the presence of the resonant response of the enclosure. This is due to aliasing effects in the Fourier transform, which is caused by the high sidelobe levels in the Fourier transform of the rectangular truncation window. The results shown in Figure 5 are the convolution of the Fourier transform of the

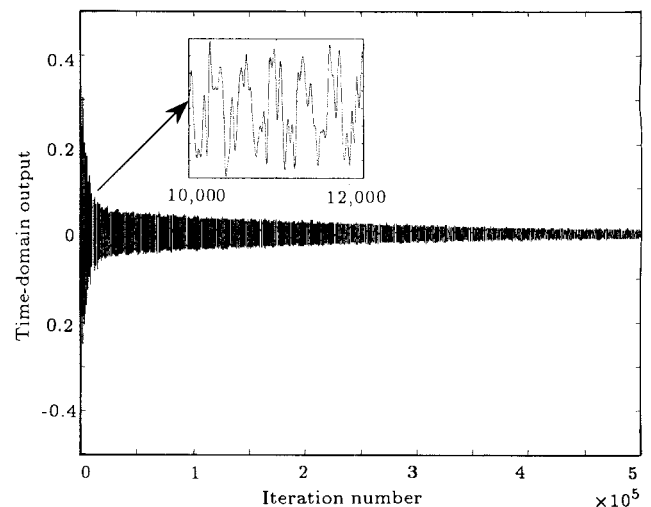


Figure 4. Time-domain output in the SE analysis of the square aperture.

rectangular window with the Fourier transform of the response shown in Figure 4.

The time domain output takes a lot of time to decay near the resonant frequency, especially for small apertures. Hence, usually a large number of time-steps is necessary for obtaining accurate results. The error and ambiguity in SE can be removed only with a large number of time-steps (more than 500,000 steps in the current case).

In order to reduce the aliasing effects, a Hanning window was applied to the time domain output, in order to reduce the number of time-steps required in the TLM method. The Hanning window considered is given by:

$$W(t) = 0.5 + 0.5 \cos(\pi t/T), \quad -T < t < T, \quad (4)$$

The width of the window, T , will be inversely proportional to the aperture size. In the simulations presented here, the computations were limited to 20,000 time steps (92 minutes of run-time) when a Hanning window was utilized. Without the Hanning window, however, at least 500,000 iterations (or 38 hours of run-time) were needed to give an acceptable result, as shown in Figure 5b. Thus, a factor of 25 improvement in

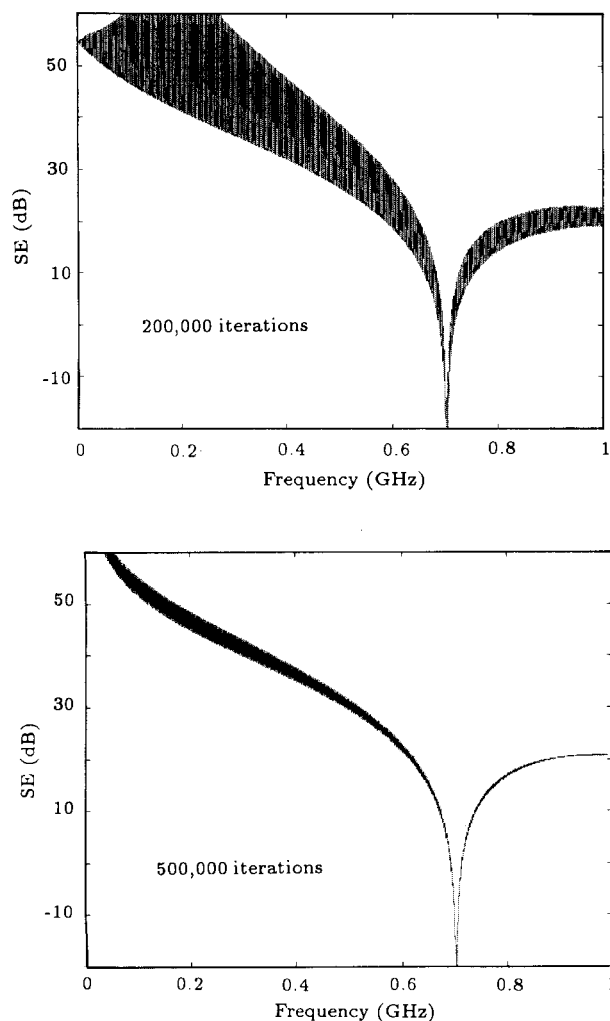


Figure 5. The SE of the square aperture obtained from the truncated output for various number of iterations (thickness $t = 2.5$ mm).

speed was achieved while the accuracy of the results was retained.

Figure 6 shows the calculated results for an aperture of width $w = 5$ mm and length $l = 100$ mm at an observation point located at the center of the enclosure ($p = 150$ mm) for two different wall thicknesses, $t = 0$ and $t = 2.5$ mm. Two hundred thousand time-steps were used in these simulations and the width of the Hanning window was chosen to be the same as that of the rectangular window. That is:

$$T_1 = 200,000, \quad \Delta t = 833ns. \quad (5)$$

The negative value of SE at the resonant frequency of the enclosure clearly implies that the field is enhanced near the resonance. For a closed rectangular metallic cavity, the resonant frequency is given by:

$$f_r = \frac{c}{2} \sqrt{\left(\frac{m}{a}\right)^2 + \left(\frac{n}{b}\right)^2 + \left(\frac{p}{d}\right)^2}, \quad (6)$$

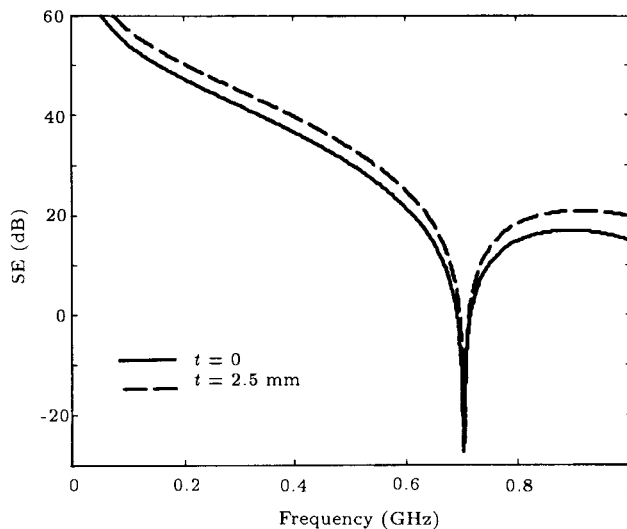


Figure 6. The SE at the center of the enclosure calculated using the Hanning window ($w = 5$ mm, $l = 100$ mm).

where c is the speed of light in free space. The dominant resonant frequency in this case is $f_r = 707.1$ MHz. In the presence of the aperture, however, the resonant frequency shifts to 702.2 MHz for $t = 0$ and to 703.7 MHz for $t = 2.5$ mm.

The above problem has been solved using the finite element method. A comparison of the results obtained from the finite element method [4], the analytical formulation of Robinson [7] and the TLM method is given in Figure 7 for $t = 1.5$ mm. The results of the TLM method for $t = 1.5$ mm was obtained by an interpolation of the two curves shown in Figure 6. It is observed that the TLM result is in better agreement with the analytical formulation of Robinson, in this case. However, this agreement should be interpreted with caution.

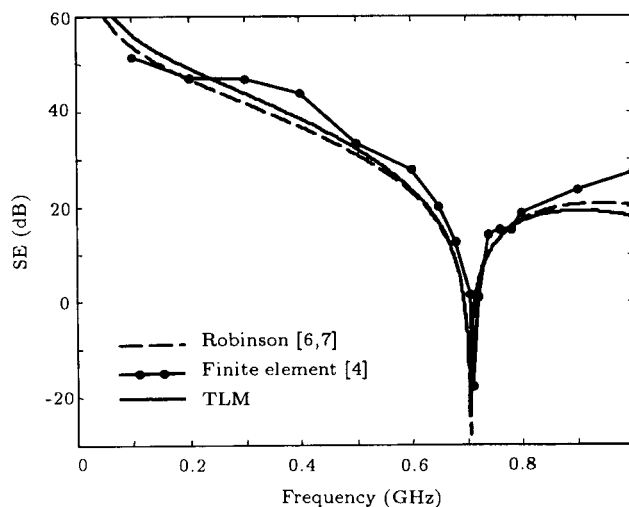


Figure 7. The SE at the enclosure center ($w = 5$ mm, $l = 100$ mm, $t = 1.5$ mm).

Robinson's formulation assumes that only the TE_{01} mode exists in the short-circuited waveguide (see Appendix). Higher order modes, however, may exist, in general, at points near the aperture and these modes may not be negligible in comparison with the dominant TE_{01} mode. To illustrate this, consider the evaluation of the SE for the previous enclosure at an observation point located at $p = 30$ mm. Figure 8a gives a comparison of the results of the TLM analysis and Robinson's formulation and, as expected, a noticeable difference is observed between the two. If the observation point is moved to a location where the next higher order mode (TE_{03}) is actually zero ($p = 30$ mm, $y = 100$ mm, say), a better agreement between the results will be observed, as depicted in Figure 8b. This shows that when higher

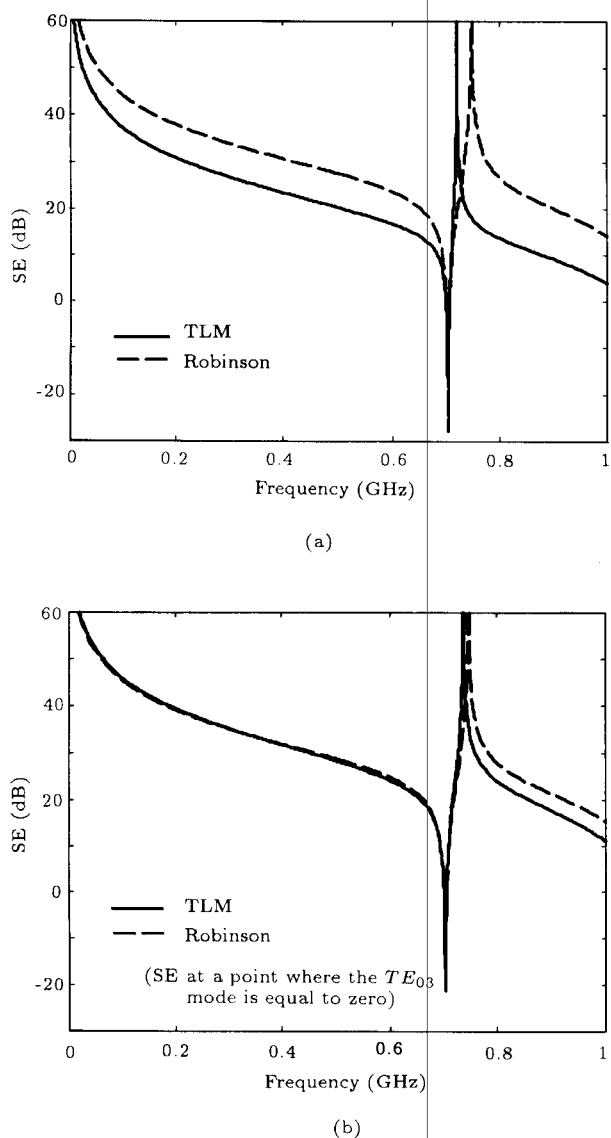


Figure 8. The SE at a point close to the aperture: $p = 30$ mm ($w = 5$ mm, $l = 100$ mm, $t = 2.5$ mm).

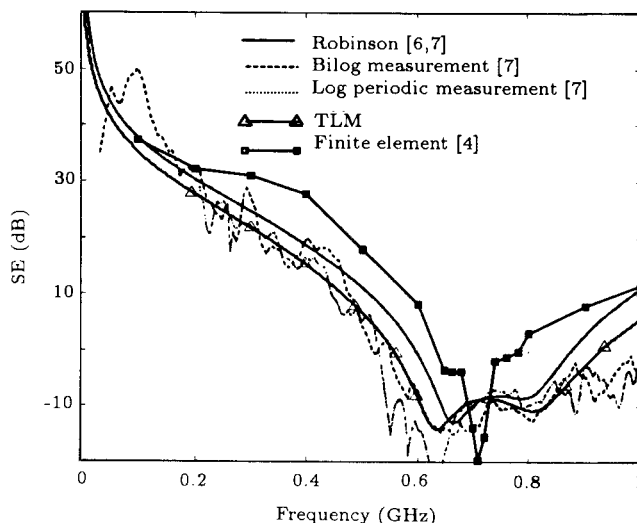


Figure 9. The SE at the center of the enclosure with a 30 mm \times 200 mm aperture.

order modes exist, the method gives more accurate results.

The shielding effectiveness of the rectangular enclosure under consideration with a larger aperture of size 30 mm \times 200 mm has been measured and reported in [7]. The wall thickness was $t = 1.5$ mm. The measurements were made by placing a sensor inside the enclosure and, also, by observing the emission from a radiating circuit within the enclosure. The field source was a network analyzer connected via an amplifier to a log periodic or bilog antenna. Figure 9 shows a comparison of the measurements with the numerical data as well as the finite element method [4] and Robinson's formulation [7]. It is observed that, in this case, the TLM method gives a better agreement with the measurements.

In the above TLM simulation, a non-uniform graded mesh was used to set the minimum cell size equal to 1.5 mm at the enclosure wall, without increasing the overall number of nodes. Because of the greater aperture size (in comparison with the previous example), a greater damping factor was observed in the time domain output. Thus, a narrower Hanning window was used ($T = 80$ ns), leading to a reduction in processing time.

EFFECTS OF APERTURE SHAPES

The shape of the enclosure aperture has a direct effect on shielding effectiveness. Here, the effects of apertures of different shapes on the SE of the same enclosure are compared.

All apertures have the same surface area. The first aperture is a rectangle of size 30 mm \times 120 mm, the second is a 60 mm \times 60 mm square aperture,

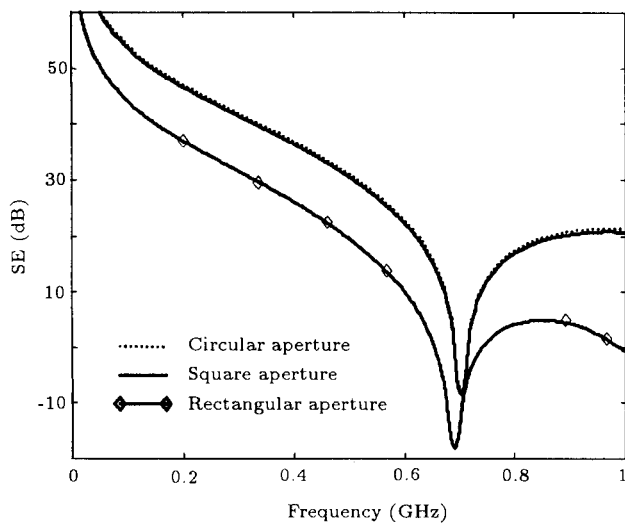


Figure 10. The SE at the enclosure center for apertures of area $S = 3600 \text{ mm}^2$.

while the last is a circular aperture of radius 33.85 mm. The wall thickness is assumed to be zero in all three cases. A uniform mesh of cell size $\Delta l = 2.5 \text{ mm}$ was used in the calculations. The computations were limited to 20,000 time steps. The run-time for each simulation was about 92 minutes on a Pentium II 450 MHz processor.

Figure 10 gives a comparison of the shielding effectiveness at the center of the enclosure ($p = 150 \text{ mm}$) for the three apertures. The same comparison is shown in Figure 11 for other observation points ($p = 30 \text{ mm}$ and $p = 270 \text{ mm}$). These results show that a circular aperture and a square aperture of the same surface area have basically the same shielding effectiveness. Also, it can be seen that the SE of a circular or square aperture is better than the SE of a rectangular aperture.

CONCLUDING REMARKS

The TLM method was used for the analysis of the shielding effectiveness of a metallic enclosure with rectangular and circular apertures. It was shown that the electromagnetic SE characterization using the TLM method, is very efficient over a wide frequency range.

Applying a simple Hanning window in the time-domain made it possible to drastically reduce the calculation time, especially in the presence of small apertures, while maintaining the desired accuracy. The proposed method can be used as an intermediate design tool for the evaluation of the effects of various aperture shapes on the effectiveness of shielded assemblies.

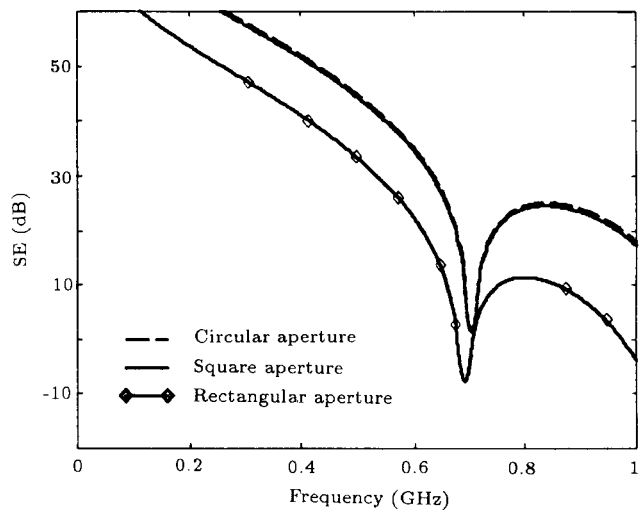
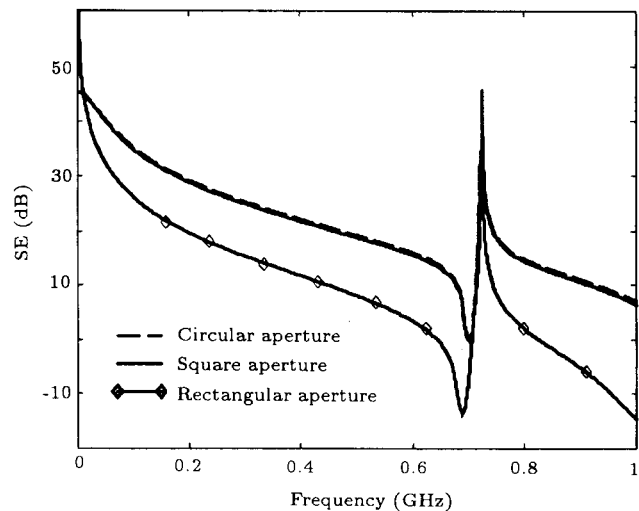


Figure 11. The SE of three apertures of the same surface area (a) $p = 30 \text{ mm}$ (b) $p = 270 \text{ mm}$.

REFERENCES

1. Christopoulos, C. "Application of the TLM method to equipment shielding problems", *IEEE International Symposium on Electromagnetic Compatibility*, **1**, pp 188-193 (1998).
2. Cerri, G., Leo, R.D., Primiani, V.M. and Righetti, M. "Field penetration into metallic enclosures through slots excited by ESD", *IEEE Trans. Electromagnetic Compatibility*, **EMC-36(2)**, pp 110-116 (May 1999).
3. Cerri, G., Leo, R.D. and Primiani, V.M. "Theoretical and experimental evaluation of the electromagnetic radiation from apertures in shielded enclosures", *IEEE Trans. Electromagnetic Compatibility*, **EMC-34(4)**, pp 423-432 (November 1992).
4. Edrisi, M. "A modeling technique for electromagnetic compatibility of enclosures in system integration and performance analysis", Ph.D. Dissertation, University of South Australia (March 2000).

5. Johns, P.B. "A symmetrical condensed node for the TLM method", *IEEE Trans. Microwave Theory Tech.*, **MTT-35**(4), pp 370-377 (April 1987).
6. Robinson, M.P., Turner, J.D., Thomas, D.W.P., Dawson, J.F., Ganley, M.D., Marvin, A.C., Porter, S.J., Benson, T.M. and Christopoulos, C. "Shielding effectiveness of a rectangular enclosure with a rectangular aperture", *Electronic Letters*, **32**(17), pp 1559-1560 (1996).
7. Robinson, M.P., Benson, T.M., Christopoulos, C., Dawson, J.F., Ganley, M.D., Marvin, A.C., Porter, S.J. and Thomas, D.W.P. "Analytical formulation for shielding effectiveness of enclosures with apertures", *IEEE Trans. Electromagnetic Compatibility*, **EMC-40**(3), pp 240-248 (1998).

APPENDIX

Robinson Formulation

Consider the enclosure as a short circuited waveguide. Assuming that only the dominant TE_{01} mode can propagate in the waveguide, the structure shown in Figure 2 can be modeled as the equivalent circuit of Figure A1. The short circuited waveguide and the aperture are represented by transmission lines. For the TE_{01} mode, the guide impedance and the guide propagation constant are given by:

$$Z_g = Z_0 / \sqrt{1 - (\lambda/2b)^2}, \quad Z_0 = 377\Omega, \quad (\text{A1})$$

$$k_g = k_0 / \sqrt{1 - (\lambda/2b)^2}, \quad k_0 = 2\pi/\lambda, \quad (\text{A2})$$

and for the aperture, the characteristic impedance

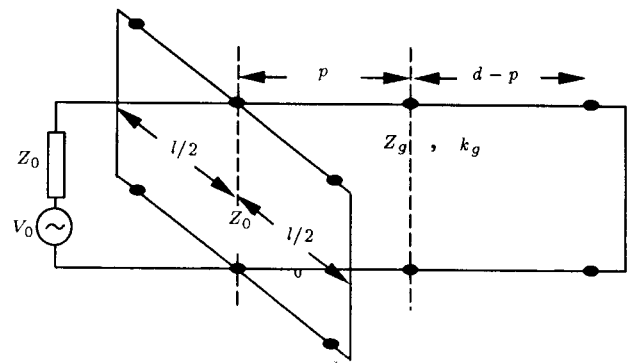


Figure A1. The equivalent circuit of Figure 2.

and the propagation constant of a coplanar strip transmission line of total width a and separation w is used. That is:

$$Z_{0s} = 120\pi \frac{K(k_e)}{K(k'_e)},$$

$$k_e = w_e/a, \quad k'_e = \sqrt{1 - k^2}, \quad (\text{A3})$$

where K is the complete elliptic integral of the first kind and the effective width, w_e , is given by:

$$w_e = w - \frac{5t}{4\pi} \left(1 + \ln \frac{4\pi w}{t}\right). \quad (\text{A4})$$

The equivalent circuit of Figure A1 can be used to find the shielding effectiveness [6,7].